J. Fluid Mech. (1986), *vol.* 170, *pp.* 169–197
Printed in Great Britain

On transition of the pulsatile pipe flow

By J. C. STETTLER† AND A. K. M. FAZLE HUSSAIN
Department of Mechanical Engineering,
University of Houston-University Park, Houston, TX 77004, USA

(Received 3 August 1983 and in revised form 27 February 1986)

Transition in a pipe flow with a superimposed sinusoidal modulation has been studied in a straight circular water pipe using laser-Doppler anemometer (LDA) techniques. This study has determined the stability–transition boundary in the three-dimensional parameter space defined by the mean and modulation Reynolds numbers Re_m, $Re_{m\omega}$ and the frequency parameter λ. Furthermore, it documents the mean passage frequency F_p of 'turbulent plugs' as functions of Re_m, $Re_{m\omega}$ and λ. This study also delineates the conditions when plugs occur randomly in time (as in the steady flow) or phase-locked with the excitation. The periodic flow requires a new definition of the transitional Reynolds number Re_{tr}, identified on the basis of the rate of change of F_p with Re_m. The extent of increase or decrease in Re_{tr} from the corresponding steady flow value depends on λ and $Re_{m\omega}$. At any Re_m and $Re_{m\omega}$, maximum stabilization occurs at $\lambda \approx 5$. With increasing $Re_{m\omega}$, the 'stabilization bandwidth' of modulation frequencies increases and then abruptly decreases after levelling off. The maximum stabilization bandwidth depends strongly on Re_m, decreasing with increasing Re_m. Previously reported observations of turbulence during deceleration, followed by a relaminarization during acceleration, can be explained in terms of a new phenomenon: namely, periodic modulation produces longitudinally periodic cells of turbulent fluid 'plugs' which differ in structural details from 'puffs' or 'slugs' in steady transitional pipe flows and are called *patches*. The length of a patch could be increased continuously from zero to the entire pipe length by increasing Re_m. This tends to question the concept that all turbulent plugs (and even the fully-turbulent pipe flow) consists of many identical elementary plugs as basic 'building blocks'.

1. Introduction

Transition from laminar to turbulent flow has for long captured the curiosity of fluid dynamicists, not only because it is a fascinating topic of unique mathematical challenge, but also because an understanding of transition may lead to its suppression and hence to a reduction of drag or to an understanding of the resulting shear-flow turbulence. In fact, an understanding of instability waves may lead to an understanding of wavelike or organized motions in turbulent shear flows, the motions being presumed to be dominated by such waves (Landahl 1967; Reynolds & Hussain 1972) and coherent structures (Roshko 1976; Cantwell 1981).

The instability of the circular Poiseuille flow continues to remain elusive both analytically and experimentally. The linearized stability problem for the fully-developed pipe flow seems to possess no finite critical Reynolds number, and therefore presumably exhibits no bifurcation point. That is, according to the linear theory, this flow is stable to infinitesimal disturbances up to infinite Reynolds

† Present address: Brown, Boveri & Cie., Abt. ZXE, CH-5401, Baden, Switzerland.

numbers (e.g. Gill 1965; Lessen, Sadler & Liu 1968; Davey & Drazin 1969; Garg & Rouleau 1972; Rosenblat & Davis 1979). A nonlinear instability theory is an obvious possibility to be considered for this flow, but it could not yet be developed in a classical way because of the lack of a neutral curve or a critical Reynolds number for infinitesimal disturbances. Analytical approaches for nonlinear instability have produced controversial results (Itoh 1977; Davey & Nguyen 1971), while direct numerical simulation (Patera & Orszag 1981) failed to reveal any instability at all. Davey & Nguyen's and Itoh's theories, based on the weakly nonlinear Stuart–Watson formalism which alters the linear stability properties of a flow field only slightly (Stuart 1960; Watson 1960), should not be expected to resolve nonlinear instability of circular Poiseuille flow because such theories are valid only near the linear neutral curve – a curve that presumably does not exist for circular Poiseuille flow. In contrast, strong nonlinear theories that can alter significantly the stability properties of a given flow appear to hold some hope for the circular Poiseuille flow. In this respect, the analyses of Benney & Bergeron (1969) and Davis (1969), which address the fully nonlinear critical layer, appear promising, even though applicable only at large Reynolds numbers. The stability of the pipe flow, therefore, continues to remain an outstanding challenge to the theoreticians. However, while pipe flows can be kept stable up to very large Reynolds numbers if care is taken to suppress disturbances, all pipe flows do become turbulent if the Reynolds number is sufficiently large. Instability in the entrance region, where the parabolic profile is not yet attained, may appear as one likely explanation for transition in practical pipe flows (Tatsumi 1952; Gill 1965); a variety of other possibilities have also been suggested (Mackrodt 1976; Hocking 1977; Smith 1979).

The analysis of Rosenblat & Davis (1979) represents a departure from the classical approaches such as the Poincaré–Hopf bifurcation theory or the Landau–Stuart–Watson (amplitude equation) formulation. Spurred by the computational results that there exists a set of disturbances whose decay rates tend to zero as the pipe Reynolds number $Re \to \infty$, they suggest that for the pipe flow, which has no bifurcation point at finite Re, the $Re = \infty$ represents a bifurcation point. This in effect claims that the pipe-flow instability is a strongly nonlinear problem (the viscous and inertia effects being comparable at $Re \to \infty$), while the classical bifurcation or instability theories as well as small-norm bifurcating solutions (e.g. Davey & Nguyen 1971; Itoh 1977) relate only to weakly-nonlinear problems. This 'birfurcation from infinity' concept appears very attractive but it is yet to be exploited theoretically or numerically to solve the pipe-flow-instability problem.

In this context, the recent theoretical analysis of circular-pipe-flow instability for non-symmetric disturbances at large Re by Smith & Bodonyi (1982) is particularly interesting. They have been able to show that neutral solutions exist for non-dimensional wavespeeds in the range 0.284–1 when the azimuthal wavenumber is 1, that the critical layer is fully nonlinear and three-dimensional and that the velocity jump and in particular the phase jump across the critical layer is small (of order $Re^{-\frac{1}{2}}$). The structure of this mainly inviscid critical layer, not unlike those studied by Benney & Bergeron (1969) and Davis (1969), is in striking contrast with either the classical linear viscous critical layer (Lin 1955; Drazin & Reid 1981) or even the nonlinear viscous critical layers studied by Haberman (1972) and Brown & Stewartson (1980). Smith & Bodonyi also infer that no similar neutral mode exists outside the wavespeed range given above. Experimental verification of these results as well as further extension of the analysis is needed.

Transition in the steady pipe flow has been the focus of many investigations

starting with Osborne Reynolds in the 1880s. Experiments by him and others (for example, Lindgren 1957; Wygnanski & Champagne 1973) showed that the transitional flow consists of turbulent regions interspersed with laminar flows. These regions, previously characterized as 'puffs' and 'slugs' (explained in §3.1), will be called 'plugs' in this paper. That is, plugs generically denote puffs, slugs, patches (discussed later) and other possible structures in pipe flows. 'Plug' will be used whenever the identification of a particular structure is unnecessary. Even though a great deal of attention has been paid to the details of puffs and some to slugs, experimental observations of transition in even the steady flow continue to raise many unanswered fundamental questions. These include questions regarding the mechanisms of entrainment, detrainment and production, and the topological details and roles of constituent sub-regions of these structures.

Far less is known about transition in an unsteady, in particular, pulsatile, pipe flow. This flow is of especial interest because of its relevance to various technological situations (for example, in Stokes layers on surfaces exposed to water waves, in pipe flows from and to positive displacement pumps, in hydraulic and pneumatic control systems, in liquid propellant rockets, etc.) and vascular flows (for example, Nerem & Seed 1972; Anliker *et al.* 1977) as well as the curiosity naturally provoked by its dynamics. In particular, an understanding of wave–wave interactions or the later stage of transition to turbulence can be facilitated by studies of instability of time-periodic flows (Greenspan & Benney 1963).

The modulated flow problem is characterized by the following non-dimensional parameters:

$$\lambda = D(\omega/4\nu)^{\frac{1}{2}} \qquad \text{frequency parameter,}$$

$$Re_{\mathrm{m}} = U_{\mathrm{m}} D/\nu \qquad \text{mean Reynolds number,}$$

$$\left.\begin{aligned} Re_{\mathrm{m}\omega} &= U_{\mathrm{m}\omega} D/\nu \\ Re_{\mathrm{c}\omega} &= U_{\mathrm{c}\omega} D/\nu \end{aligned}\right\} \qquad \text{modulation Reynolds numbers,}$$

$$\Delta = U_{\mathrm{m}\omega}/U_{\mathrm{m}} = Re_{\mathrm{m}\omega}/Re_{\mathrm{m}} \qquad \text{modulation velocity amplitude,}$$

$$F_{\mathrm{p}} = f_{\mathrm{p}} D/U_{\mathrm{m}} \qquad \text{plug passage frequency,}$$

where D is the pipe diameter; $\omega\,(=2\pi f_{\mathrm{p}})$ is the circular frequency of pulsation; U_{m} is the time-mean of the cross-sectional average velocity $U_{\mathrm{m}}(t)$; $U_{\mathrm{m}\omega}$ is the modulation amplitude of $U_{\mathrm{m}}(t)$; $U_{\mathrm{c}\omega}$ is the velocity modulation amplitude at the centreline; and ν is the kinematic viscosity. For a discussion of analysis and experiments in pulsatile laminar and turbulent flows, see Hussain (1977).

The periodic modulation can stabilize the flow since periodic modulation introduces a displacement effect reducing the effective diameter of the more instability-susceptible core flow and hence reducing the effective Reynolds number, Re (Davis 1976). That is, when modulated appropriately, the flow Re can be increased in practice without causing transition, so that the effective Re (and not the pipe Re) is indeed the transitional Reynolds number. (This modulation-induced stabilization is not unlike the stabilization of an inverted pendulum brought about by oscillating the fulcrum.) On an independent basis, modulation also can destabilize the flow since modulation produces inflectional profiles which are inviscidly unstable according to the Rayleigh criterion (see, for example, Lin 1955; Drazin & Reid 1981). However, the modulation-induced Stokes layer has been found to be stable to infinitesimal disturbances (von Kerczek & Davis 1974) and hence disallows the development of a nonlinear theory (because of the unavailability of a critical Reynolds number based

on the linear theory). It is interesting to note that Davis (1976) speculated that the stability of the inflectional profile in a periodic flow was due to the fact that too short a time was allowed for the growth to manifest itself before the basic state was modified. That is, he suggested that if the frequency is low, inflectional profiles will be unstable, as is to be expected from the Rayleigh criterion. This provocative speculation has remained untested. It is worth noting that Tozzi's (1982) computation failed to show instability due to inflectional profile in a pipe.

Among time-dependent flows with a non-zero mean velocity, the plane Poiseuille flow has been most widely studied theoretically. This flow should also be relevant to unsteady pipe flow, as the wall curvature can be neglected if the Stokes layer thickness is much smaller than the pipe radius (i.e. at high frequencies). In general, theoretical and numerical studies (for example, Grosch & Salwen 1968; Herbert 1972; Hall 1975; von Kerczek 1982) have predicted stabilization of the flow due to periodic modulation. Hall and von Kerczek independently showed that very high oscillation frequencies destabilized the plane Poiseuille flow. Von Kerczek found a slight destabilization at very low modulation frequencies. At intermediate oscillation frequencies the results of Grosch & Salwen and von Kerczek strongly disagree. Whereas Grosch & Salwen predict an abrupt destabilization of the flow at high amplitudes of modulation ($\Delta > 0.105$), von Kerczek dismisses this prediction as 'unlikely' on the basis of theoretical analysis valid for $\Delta \leqslant 0.25$.

Very limited theoretical work has been done on the stability of oscillating circular Poiseuille flow. Tozzi (1982) found a modulation-induced stabilization of the flow up to very high modulation amplitudes. This is not in accord with experimental results, which show a destabilization of the flow even at comparatively lower Δ.

The stability of periodic pipe flow has been experimentally studied by a number of researchers. Instability of a sinusoidally modulated pipe flow with zero mean has been investigated by Merkli & Thomann (1975), Sergeev (1966) and Hino, Sawamoto & Takasu (1976). Sergeev found a linear increase of the critical Reynolds number with increasing λ. Merkli & Thomann found that turbulence occurs in the form of periodic bursts which are followed by relaminarization in each cycle.

Instability of periodic pipe flow with non-zero mean flow has been investigated by Gilbrech & Combs (1963), Sarpkaya (1966) and Yellin (1966). Of these, Sarpkaya's study is the most comprehensive, but covered only a limited λ range, namely, $4 \leqslant \lambda \leqslant 7.8$. He found that the flow modulation had a considerable effect on the critical Reynolds number Re_{cr}, defined as that value of Re_{m} above which disturbances, artificially induced in the fully-developed region, grew downstream. His steady flow remained laminar up to $Re_{\mathrm{m}} = 6500$. His experiments thus show the effect of flow modulation on the growth of artificially created disturbances over the λ range 4–7.8. The present paper investigates the effect of sinusoidal oscillations on the survival of turbulent patches formed naturally from highly disturbed pipe inlet for a much larger frequency range, namely, $1 < \lambda < 70$.

The effects of flow modulation on fully-turbulent flow at low mean Reynolds numbers was investigated by Shemer & Wygnanski (1981) and Ramaprian & Tu (1980); the latter also did a few experiments at transitional Reynolds numbers.

In none of the studies on transition in unsteady pipe flow with a non-zero mean Reynolds number have the laminar–transition boundaries in the three-dimensional (Re_{m}, $Re_{\mathrm{m}\omega}$, λ) space been determined. This work primarily provides the much needed laminar–transition boundaries which are likely to be helpful toward an understanding of this fundamental problem and perhaps toward development/validation of an instability theory of pulsatile pipe flow.

Turbulent plugs like puffs and slugs are not well understood even in steady pipe flow, and very little is known about the effect of flow modulation on the structure of such plugs. In this paper, we also discuss turbulent plugs in the transitional unsteady pipe flow; further quantitative details of their topological features are being explored in a separate study (Stettler, Zaman & Hussain 1986).

2. Apparatus and procedures

The experiments were carried out in a Plexiglas pipe of diameter $D = 2.54$ cm and a total length of approximately $550D$ (see figure 1*a*). The pipe was assembled from 8 individual pieces, which were faced squarely on a lathe and joined together by Plexiglas slip couplings. Water entered the pipe from a constant head tank through a bell-shaped contraction, followed by an orifice plate (in order to induce a highly disturbed entry flow) having an opening of 1.2 cm in diameter. The location of the orifice plate identifies the origin (i.e. $x = 0$) of the longitudinal coordinate. The data presented in this paper (figures 4, 8 and 9) and thus the laminar–transition boundaries (figures 11–16) proved to be independent of the nature of the entry roughness. The F_p *vs.* Re_m curves in figures 4, 8 and 9 were reproduced for various entry conditions, namely; a small disc suspended at the pipe centre, a circular cylinder placed perpendicular to the pipe at inlet, and an orifice plate with a smaller diameter.

Measurements were made primarily at $x/D = 330$, with a few at $x/D = 16$, 45 and 110. These latter stations were investigated mainly to document the flow evolution along the length of the pipe. At $x/D = 330$, the flow is free from the effects of non-axisymmetry of the periodic opening at the downstream end of the pipe as well as any possible asymmetry of the entry flow. Thus, the flow is both axisymmetric and fully developed as confirmed by the agreement of the profile measured via LDA with the theoretical Poiseuille flow profile (figure 1*d*). (Comparison of the unsteady flow profiles with theoretical profiles will be discussed by Stettler *et al.* 1986.) The large obstruction at the pipe exit minimized the effect of the relative fraction of laminar and turbulent flows inside the pipe on the total pressure drop; the flow was therefore not self-regulated. At the downstream end of the closed pipe, a narrow rectangular slot was cut into the pipe wall. A sinusoidal flow modulation with a non-zero mean was obtained by rotating a sleeve (with its end cut at a certain angle, see figure 1*c*) which periodically covered and uncovered the slot, thus opening and closing the exit cross-section sinusoidally; see Schultz-Grunow (1940). A d.c.-motor with a variable speed control was used to rotate the sleeve at selected speeds. Care was taken to ensure negligible harmonic content of the modulation. To this end, the frequency spectrum of the longitudinal velocity signal at the pipe centreline was determined for laminar flow at each excitation condition. The amplitude of the first harmonic was always less than 5% of the fundamental, with no detectable higher harmonics.

A 35 mW He–Ne laser in conjunction with a counter-type signal processor (TSI Model 1990) was used in the dual-beam forward-scattering mode (see figure 1*b*) to obtain the longitudinal velocity signal. The focal length of both the focusing and receiving lenses was 120 mm, which resulted in a length of the major axis of the measuring volume of approximately 1 mm. This comparatively large size of the measuring volume was not critical in our experiments, as we were primarily interested in detecting turbulent plugs in between laminar flows. Frequency shifting of one laser beam was employed to optimize the filter setting of the LDA counter

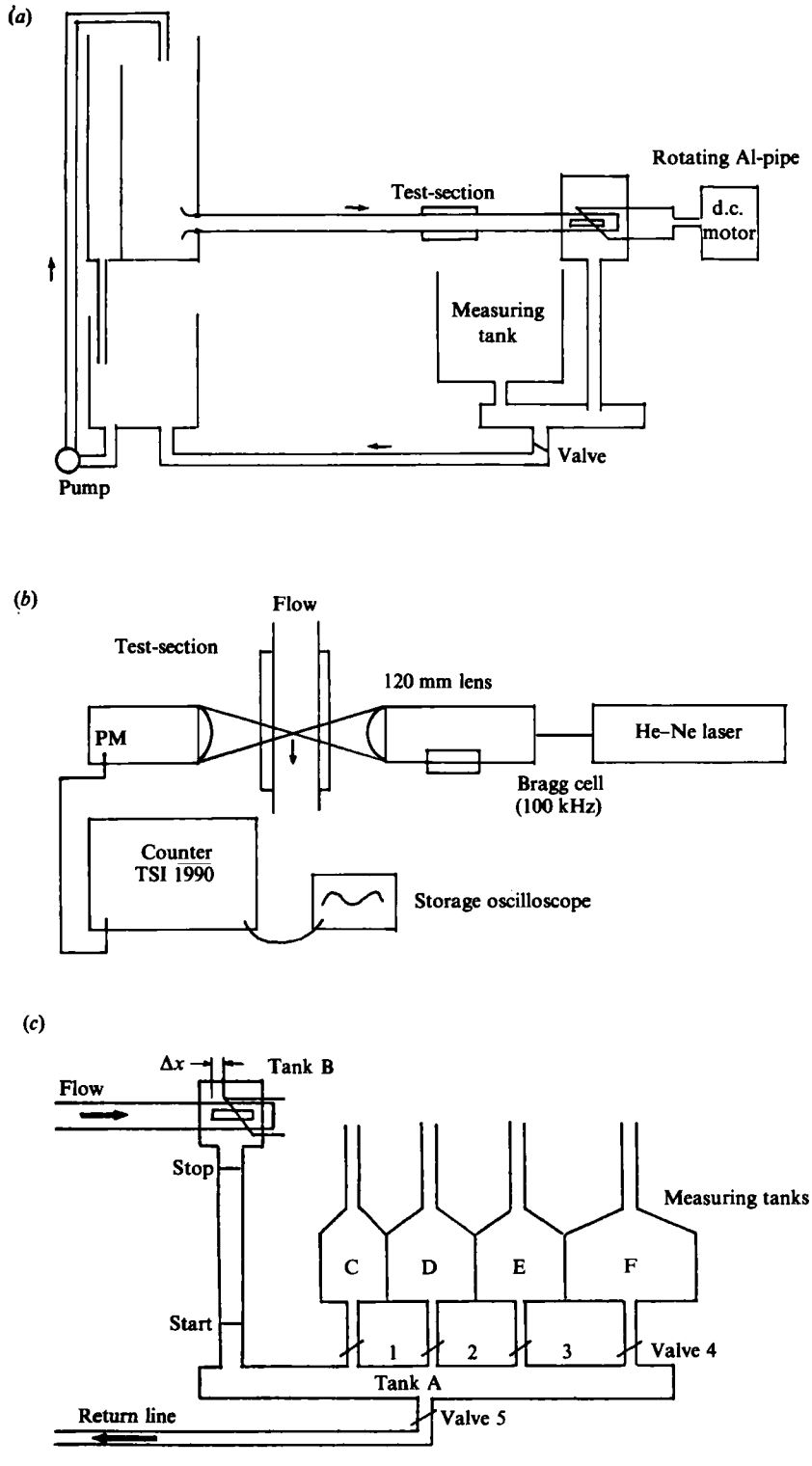

FIGURE 1(*a–c*). For caption see facing page.

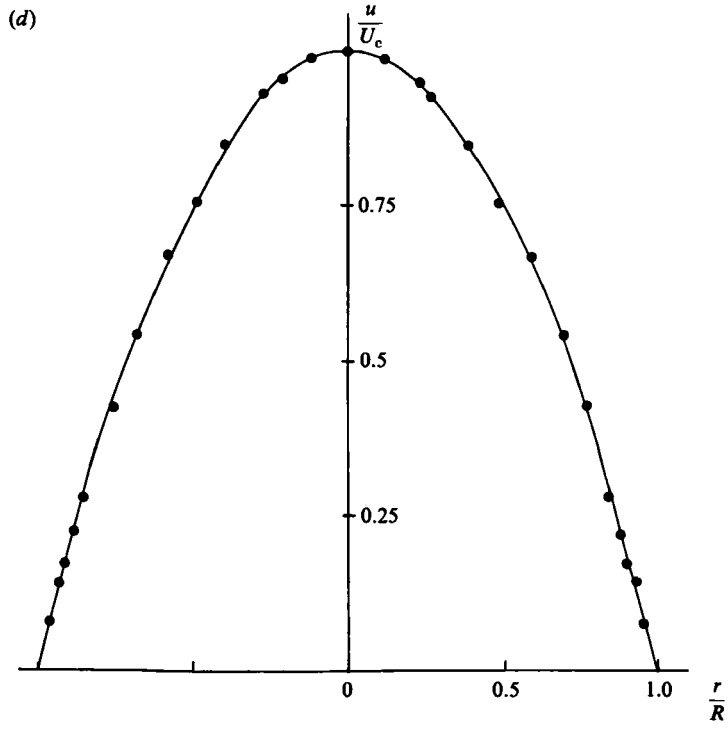

FIGURE 1. (*a*) Schematic of the flow facility; (*b*) LDA system set-up; (*c*) Schematic of the pulsation device at the pipe exit and measuring tanks to determine the flow rate; (*d*) Longitudinal velocity profile measured with the LDA-system and compared with the Poiseuille profile (line).

in order to remove the pedestal and high frequency noise, as well as to detect flow reversal. (The counter was operated in manual, N-cycle mode with $N = 8$ for most cases.) The LDA system rested on a table whose top plate could be traversed with a backlash-free traversing mechanism. The axial velocity could, therefore, be easily measured for different radial and axial locations, without realigning the optical system at each measuring point. Natural seeding of the water was enough to ensure a continuous velocity signal of the analog output of the counter. The temperature of the water was kept constant (24 °C) to ensure a constant value of the viscosity.

2.1. *Measurement and alteration of* Re_m, $Re_{m\omega}$ *and* λ

A series of calibrated tanks with START and STOP marks on narrow pipes above and below the tanks (to assure accurate measurements of filling times) were used to measure the mean Reynolds number Re_m. By having the four valves (1–4) in figure 1(*c*) either open or closed (in various combinations), the actual measured volume could be optimized to minimize the measuring time without sacrificing accuracy. The frequency ω of flow modulation was measured from the time period for an integral number of cycles, and $U_{c\omega}$ (and thus $Re_{c\omega}$) was obtained from the centreline velocity traces on a storage oscilloscope.

Since transition in a practical pipe flow occurs in the form of random turbulent plugs travelling down the pipe, $Re_{c\omega}$ will vary depending on whether it is measured for a period of laminar flow or a period of turbulent flow. At the onset of transition, however, the flow is fully laminar most of the time, and we defined $Re_{c\omega}$ with $U_{c\omega}$ measured for a period of laminar flow. When the slot is fully covered, $U_{m\omega}$ becomes

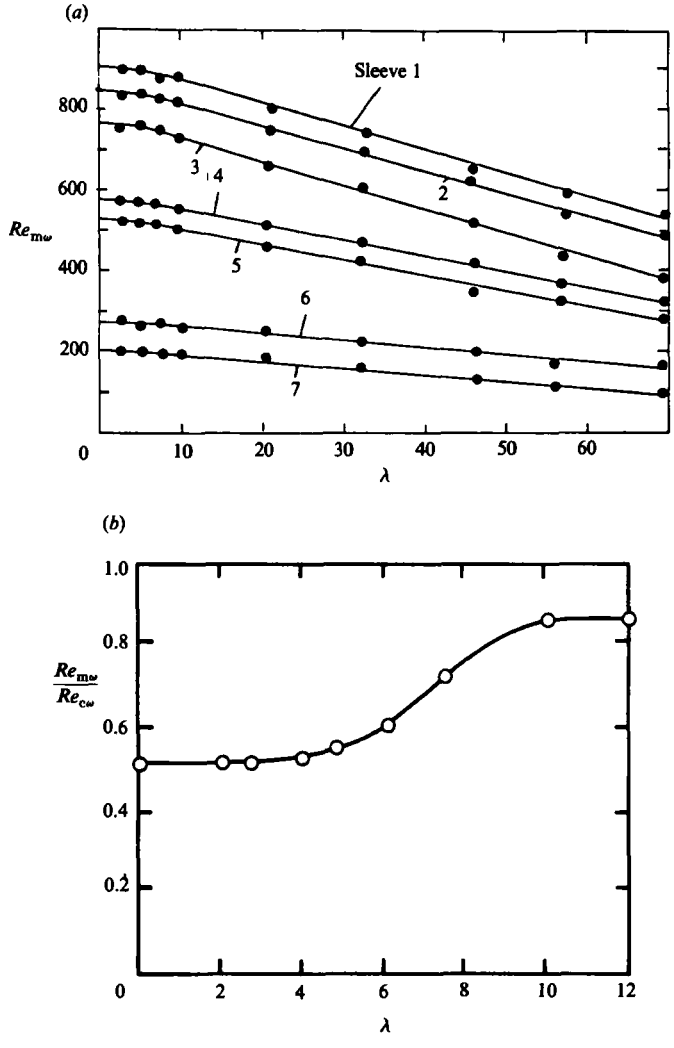

FIGURE 2. (*a*) $Re_{m\omega}$ *vs.* λ calibration curves for 7 different sleeves; (*b*) Ratio between modulation amplitudes of the cross-sectional-mean velocity and the centreline velocity, $Re_{m\omega}/Re_{c\omega}$, as a function of λ.

equal to U_m and, thus, can be measured as discussed. Our experimentally obtained $Re_{m\omega}/Re_{c\omega}$ *vs.* λ curve in figure 2(*b*) shows that $Re_{m\omega}/Re_{c\omega}$ is strongly λ-dependent only for $3 < \lambda < 10$ (Uchida 1956).

The modulation amplitude could be varied by changing the exit slot at the downstream end of the Plexiglass pipe and/or by changing the sleeve angle (figure 1*c*). Due to the inertia effect of the water column inside the $550D$ long pipe, an increase in λ reduced the modulation amplitude. Figure 2(*a*) indicates the nature of the $Re_{m\omega} - \lambda$ relationship used as calibration curves for a few sleeves; these were used to set selected operating points $(Re_{m\omega}, \lambda)$. The Re_m value could easily be varied by changing the relative displacement Δx of the sleeve with respect to the slot opening (see figure 1*c*), and the frequency parameter λ was varied by controlling the voltage to the d.c.-motor. Note that $Re_{m\omega}$ decreased monotonically with increasing λ for each sleeve.

3. Results and discussion

3.1. *Transition in steady pipe flow*

Before studying the modulated pipe flow, the steady flow and its transition characteristics were investigated first. A well-defined transition regime exists for the steady pipe flow with a highly disturbed entrance. For Re_m between 2000 and 2700, the pipe flow consists of longitudinally separated regions of turbulent plugs called puffs. These differ from slugs which were first reported by Osborne Reynolds to occur in a somewhat higher Reynolds number range. There have been speculations in the past about the various possible turbulent structures that may occur in the steady pipe flow at transitional Reynolds numbers; see, for example, Morkovin (1977). Various attempts were made to classify them into puffs and slugs, but a clear definition is still lacking. For instance, Coles (1981) calls puffs those turbulent plugs that occur when the entry flow is highly disturbed and Re_m is between 2000 and 2450. In this Re_m-range, succeeding puffs are clearly separated by laminar flow. At higher Reynolds numbers ($2400 < Re_m < 2700$) turbulent fluid plugs start to merge and interact with each other. Wygnanski & Champagne (1973) refer to these larger structures also as puffs; they classify structures strictly in terms of origin: puffs for disturbed entry, and slugs for instability of the developing region boundary layer. Rubin, Wygnanski & Haritonidis (1980) claim that slugs result from coalescence of puffs.

Based on our own detailed observations of transition in steady and unsteady pipe flows, we prefer the more restrictive definition of Coles. Slugs seem to originate from (Tollmien–Schlichting) instability waves of the entry region boundary layer. On the other hand, puffs are debris of relaminarization of fully-turbulent flow induced at the entry by large disturbances or roughness (which can be an orifice, grid, disc, etc.). Puffs consist of a sharp upstream front and a long (20–30 diameters) quiescent downstream region over which turbulent fluid is detrained and relaminarized (Bandyopadhyay & Hussain 1985). The upstream boundaries (i.e. back) of slugs appear to be similar to those of puffs – involving breakdown of upstream laminar fluid 'jetting into' the turbulent region – but the downstream boundaries (i.e. front) of slugs involve intense large-scale vortex entanglement, laminar fluid engulfment, and breakdown (Leitko & Hussain 1983). It should be emphasized that the backs of puffs and slugs and the fronts of slugs, even though sharp, are not flat smooth surfaces perpendicular to the pipe axis, but are highly contorted interfaces occupying a few diameters in streamwise extent.

Figure 3(*a*) shows the characteristic 'footprint' of a turbulent puff in steady flow. The slow drop in centreline velocity, as the front (at smaller time) is approached, is a result of the change of the velocity profile, from a parabolic one for laminar flow downstream of the puff, to a fuller profile for turbulent flow inside the puff; of course, close to the wall, the axial velocity will rise within the puff. The transition between the turbulent interior and the laminar exterior flow at the front of the puff is gradual, whereas the back (at larger time) is very sharp. This is typical of a puff. In contrast, the front and back (i.e. leading and trailing) interfaces of a slug are equally sharp. The velocity trace in figure 3(*a*) furthermore shows that the turbulence intensity is high close to the trailing end. This is associated with roll-up and breakdown of laminar fluid jetting into the slower-moving turbulent puff; this jetting action produces a roll-up and subsequent breakdown into turbulence. This inviscid production is the mechanism for indefinite sustenance of the 'equilibrium puff' (Bandyopadhyay & Hussain 1985). Due to the absence of any production

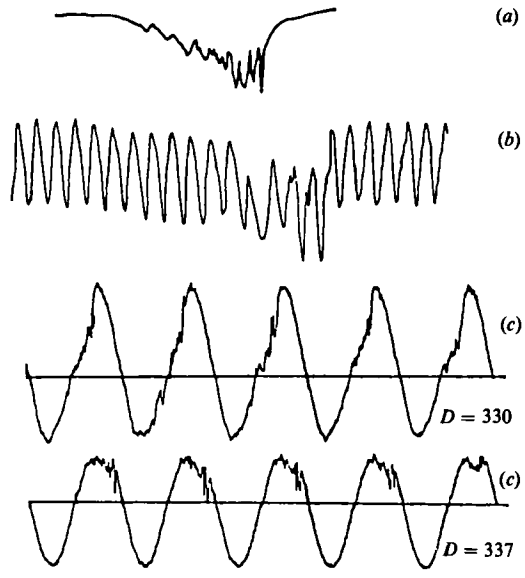

FIGURE 3. Centreline velocity signals in steady and unsteady transitional pipe flows at $x/D = 330$. (*a*) Random puff in steady flow, $Re_m \simeq 2100$; (*b*) Random puff in unsteady flow, $Re_m \simeq 2100$; $Re_{m\omega} = 600$; $\lambda = 21$; (*c*) Phase-locked turbulent 'patch' at $x/D = 330$ and $x/D = 337$, $Re_m = 1760$, $Re_{m\omega} = 1410$, $\lambda = 10$.

mechanism after breakdown, turbulence decays gradually, and the turbulent fluid relaminarizes at the front.

The gradual change of the turbulence intensity at the front of a puff makes the detection of the front interface and the measurement of the intermittency factor (i.e. the percentage of time the flow is turbulent), for transitional flow with highly disturbed entry, both imprecise and subjective. On the other hand, the average passage frequency f_p of the plugs can be measured fairly accurately, especially at lower Re_m ranges.

For steady flows, no turbulent plug was observed for Re_m below 2000. This is in general agreement with the literature (Lindgren 1957; Wygnanski & Champagne 1973), even though Ramaprian & Tu (1980) observed transition at $Re_m = 1750$ and fully turbulent pipe flow at $Re_m = 2000$. Figure 4 shows that, for $2000 \leqslant Re_m \leqslant 2350$, the non-dimensional plug frequency $F_p (\equiv f_p D/U_m)$ increases linearly with Re_m i.e. $F_p \propto (Re_m - 2000)$ until F_p reaches a maximum value at $Re_m \cong 2350$. As Re_m is further increased, F_p progressively decreases until $Re_m \simeq 2700$, above which the flow becomes fully turbulent. This decrease in F_p for higher Re_m values is due to the fact that successions of plugs merge forming larger plugs. Thus, the plug count is somewhat ambiguous at higher Re_m. The differences at higher Re_m between the present F_p data and those reported by Wygnanski & Champagne (also shown in figure 4) are therefore not of any obvious significance in the context of the present paper.

The important and often-raised question (see Coles 1981) of reproducibility among the various experiments can therefore, at least for steady flow conditions, be answered satisfactorily. Inadequate data in the literature on unsteady flow transition prevent us from comparing our data with any other. However, unsteady flow data presented in this paper proved to be repeatable over a period of two years; note that

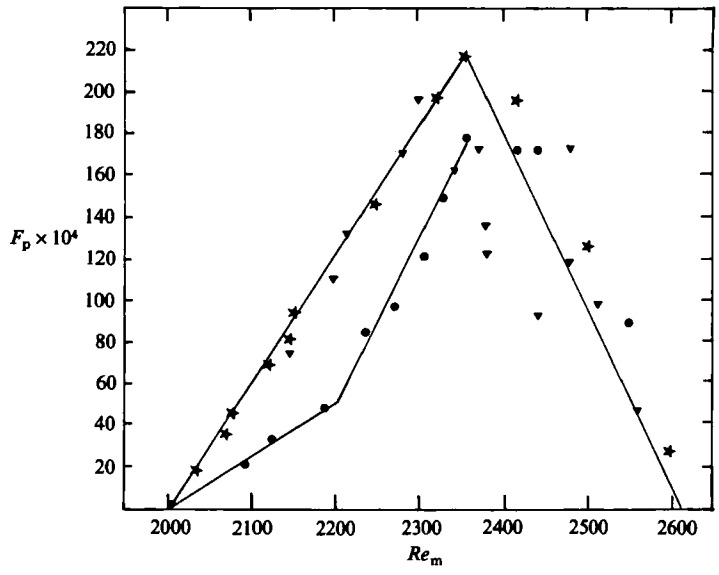

FIGURE 4. Passage frequency of turbulent puffs at $330D$ downstream. *, steady flow; ●, unsteady flow ($\lambda = 10$, $Re_{m\omega} = 565$); and ▼, steady flow data of Wygnanski & Champagne (1973).

Ramaprian & Tu (1980), for example, had problems in reproducing their data. As already mentioned, our data proved to be independent of the entrance disturbance as long as Re_{tr} of the steady flow was 2000. The effect of flow modulation on transition with streamlined entry (for which $Re_{tr} > 2000$ for steady flow) will be investigated in a later study.

3.2. *Transition in pulsatile pipe flow*

LDA signals at the pipe centreline capturing turbulent plugs in pulsatile flows at $x/D = 330$ are shown in figures 3 (*b*–*c*) and at $x/D = 337$ also in figure 3 (*c*). At a high frequency, say, $\lambda > 10$, and moderate modulation amplitudes, say, $Re_{m\omega} \lesssim 1200$, the turbulent plugs occurred randomly in time, similar to the case in steady flow. Likewise in a steady flow puff, the front of the plug is not well defined and the trailing end is quite sharp. Note that for large λ values, the decrease in the velocity from the front to the back is quite gradual, occupying several oscillation periods (figure 3*b*). In this study no attempt is made to investigate in detail the turbulent structure inside the plug. A velocity drop (at the pipe centreline) is still detectable, as the plug passes by. At high λ values, however, this velocity defect is not as distinct as in the case of puffs in steady flow. This is quite likely to be due to the fact that the profile in the laminar part (at high λ values) is flatter and not pointed like the Poiseuille profile (see Uchida 1956), so that the 'jetting action' is weakened or eliminated. High λ values combined with high modulation amplitudes lead to flow conditions where the plugs occur phase-locked with the flow modulation (figure 3*c*). These phase-locked plugs in modulated flow are termed by us as 'patches' (further discussed later).

A separate study (Stettler *et al.* 1986) shows that the structure inside a turbulent plug when it occurs phase-locked with the flow modulation (figure 3*c*) is quite different from that in a steady flow puff, which has been mapped via ensemble average data by Wygnanski, Sokolov & Friedman (1975) and visualized by Bandyopadhyay & Hussain (1985). For the patches observed at low frequencies, say, $\lambda < 4$,

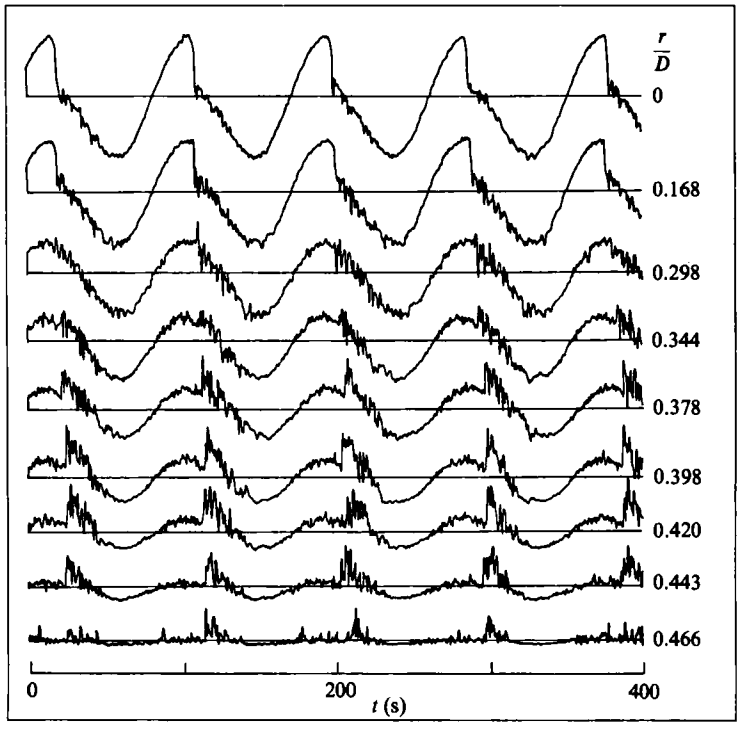

FIGURE 5. Longitudinal velocity traces at various radial positions for a phase-locked turbulent 'patch' at $x/D = 330$; $\lambda = 3.5$; $Re_m = 3840$; $Re_{m\omega} = 1400$.

the centreline velocity defect again becomes more noticeable (figure 5). The drop in the velocity as the structure approaches is abrupt, indicating a sharp leading front. This contrasts with the steady flow puff where the velocity drop at the front is very gradual (figure 3*a*). The trailing (back) interface in figure 5 is not well defined, and the high turbulence intensity at the back of the typical puff or slug is also missing. Thus, the signature of the patch is quite different from that of the puff and the slug. The velocity traces shown in figure 5 also indicate that the highest turbulence intensity does not occur on the centreline as in a puff. (The fluctuation amplitude at the centreline is noticeably lower than at $r/D \approx 0.4$ where there seems to be some small-scale turbulence even outside the patch.) Note that the downstream front is the sharpest at the centreline. Nearer to the wall, there is some turbulence activity even before the front arrives.

The difference between a patch and a puff is further documented in figure 6, which shows velocity signals of a steady-flow puff and a phase-locked patch after the signals have been high-pass filtered (to remove lower-frequency velocity undulations and thus accentuate the footprint of the fine-scale turbulence in the two structures). Note that in the pulsatile flow, turbulence on the centreline increases much more abruptly near the downstream front of the patch (figure 6*b*) as opposed to the case of puff (figure 6*a*), where turbulence is concentrated near the back (upstream end). Figure 6(*c*) shows that, as opposed to the situation in a puff, the turbulence level in a patch is higher closer to the wall.

For values of λ and $Re_{m\omega}$ comparable to those in figure 5, oscilloscope traces obtained at low Re_m values are shown in figures 7(*a–d*). At these low Re_m values, turbulence does not occur in every cycle; several modulation cycles of fully laminar

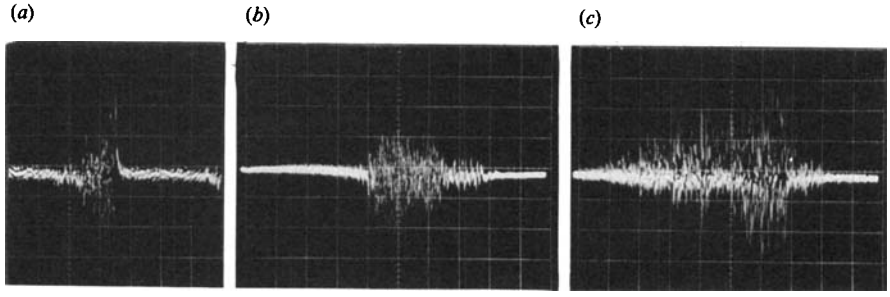

FIGURE 6. Longitudinal velocity signatures of turbulent 'plugs' after high-pass filtering: (*a*) on centreline of a turbulent 'puff' in steady flow; (*b*) phase-locked turbulent 'patch', ($\lambda = 4$, $Re_m = 3000$, $Re_{m\omega} = 1400$) at the centreline; (*c*) same as case (*b*) but close to the wall ($r/D = 0.47$).

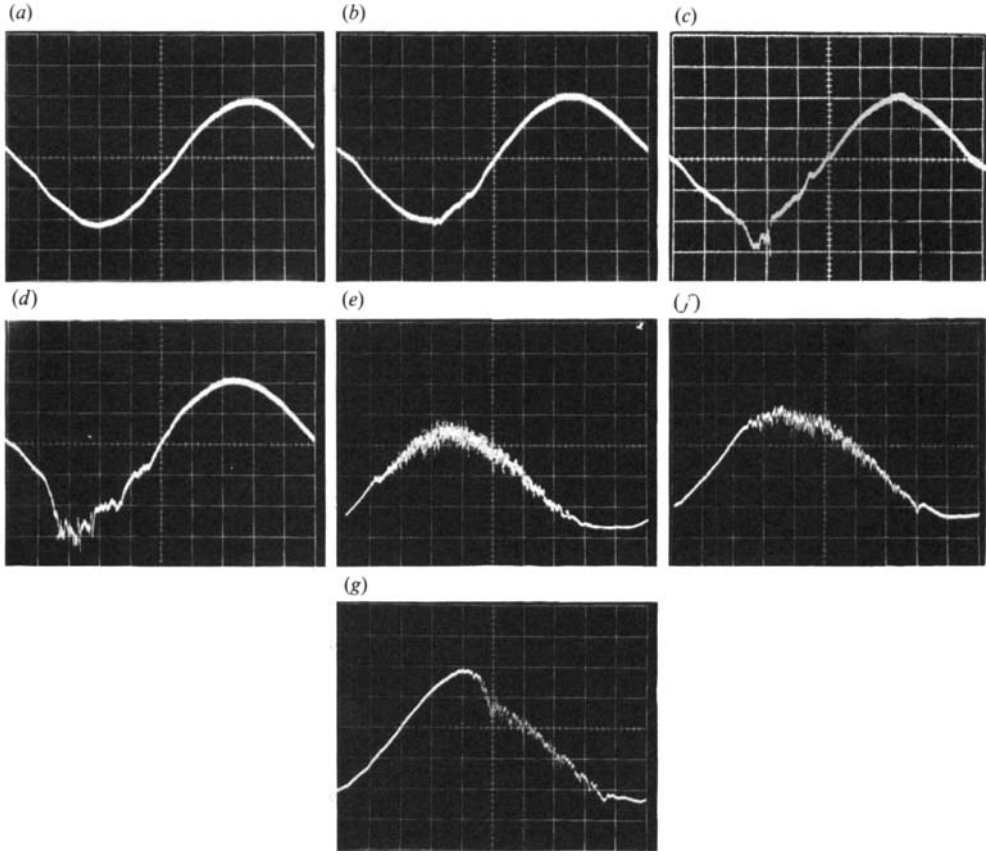

FIGURE 7. (*a*)–(*d*) Centreline velocity traces showing turbulent 'patches' of increasing length with increasing Re_m for low-frequency oscillation. (*a*) $Re_m \simeq Re_{tr}$; (*b*) $Re_m = Re_{tr} + 25$; (*c*) $Re_m = Re_{tr} + 50$; (*d*) $Re_m = Re_{tr} + 80$. (*e*)–(*g*) Same turbulent patch observed at increasing distances from the pipe inlet: ($\lambda = 4$; $Re_m = 2050$; $Re_{m\omega} = 2050$); (*e*) $x/D = 16$; (*f*) $x/D = 45$; (*g*) $x/D = 110$.

flow are possible between two succeeding plugs. This made it somewhat difficult to 'capture' the signature of such a plug. Rubin *et al.* (1980) speculated that the equilibrium puff may be a basic building block in a fully developed pipe flow. Figures 7 (*a–d*) clearly show that for transition in unsteady pipe flow, no 'basic block' of a

minimum length exists out of which all possible turbulent plugs may be created through superposition and mutual interaction. To the contrary, the increase of the plug length with increasing Re_m is very gradual from zero to the entire length of the pipe. In addition, as figure 5 shows, turbulence at higher Re_m occurs truly phase locked with the flow-modulation. Clearly, steady and unsteady flow transitions are different; our study of pulsatile flow, which allows control of the plug length to any selected value, throws some doubt on the building-block concept.

Velocity traces at increasing distances from the pipe entry are depicted in figures 7(*e–g*). (Traces from a downstream station, for instance $x/D = 330$, do not differ much from those taken at $x/D = 110$.) We found that depending on the values of Re_m, $Re_{m\omega}$ and λ, a turbulent 'plug' may shrink or grow in length for roughly the first 100 pipe diameters. After that, it reaches something of an equilibrium state with its length remaining unchanged. This conclusion was further strengthened by measuring f_p for some steady and unsteady flow conditions at $x/D = 110$. It turned out that for the flow conditions investigated, this frequency did not decrease with increasing x/D as Rotta (1956) concluded, but rather it remained constant, in agreement with Wygnanski & Champagne's (1973) observations.

From figures 3, 5 and 7 it is clear that turbulent plugs occur at different phases of the modulation period, depending on x/D, λ or Re_m. This interesting phenomenon has not been reported in the literature. We have observed that the entire flow inside the pipe does not spontaneously break down into turbulence during deceleration followed by a relaminarization during the acceleration of the flow, as has been claimed by several investigators (Yellin 1966; Shemer & Wygnanski 1981). Of course, the concept of a periodic breakdown into turbulence followed by a relaminarization of the entire flow inside the pipe is difficult to support, as the timescale for the destruction of the turbulent energy (via dissipation) is typically much larger than the typical period of oscillation. To the contrary, our observations (figures 3, 5, 7) indicate periodic creation of turbulent patches at the pipe entry (figure 7*e*). These patches are then convected down the pipe at their own celerity. The turbulent patches are detected at larger x/D at later phases in the cycle. Thus patches occur in longitudinally periodic cells separated by laminar flow. The phase locked turbulent patches are of special interest; detailed eduction of various coherent quantities and structural details can be made easily, using well-established phase-averaging techniques (Stettler *et al.* 1986; Hussain 1977). The difficulties in educing structural details in randomly occurring puffs and slugs in steady-flow experiments are considerably greater.

Figure 4 also shows the average plug frequency F_p as a function of Re_m for a sinusoidally modulated flow. For $Re_m < 2350$, the F_p values for modulated flow are lower than those for steady flow, and the F_p *vs.* Re_m curve consists of two linear regions with a sudden change in the slope at $Re_m \approx 2200$. For $Re_m > 2350$, F_p does not seem to be affected by the flow modulation. Due to the puff-count ambiguity at these high Re_m values (mentioned earlier), however, a possible effect of the flow modulation on F_p can neither be confirmed nor excluded. We restricted our study to the influence of a harmonical flow modulation on the onset of transition in situations where F_p can be determined unambiguously (figures 8, 9).

Figures 8(*a–d*) show the plug frequency F_p as a function of Re_m for different values of $Re_{m\omega}$ and λ. In general, for a given modulation frequency, the plug frequency F_p decreases with increasing amplitude of modulation. For all modulation amplitudes documented in figure 8(*a*), the turbulent plugs occurred randomly in time. At this relatively high λ value, the lock-in of turbulence with the modulation period (when

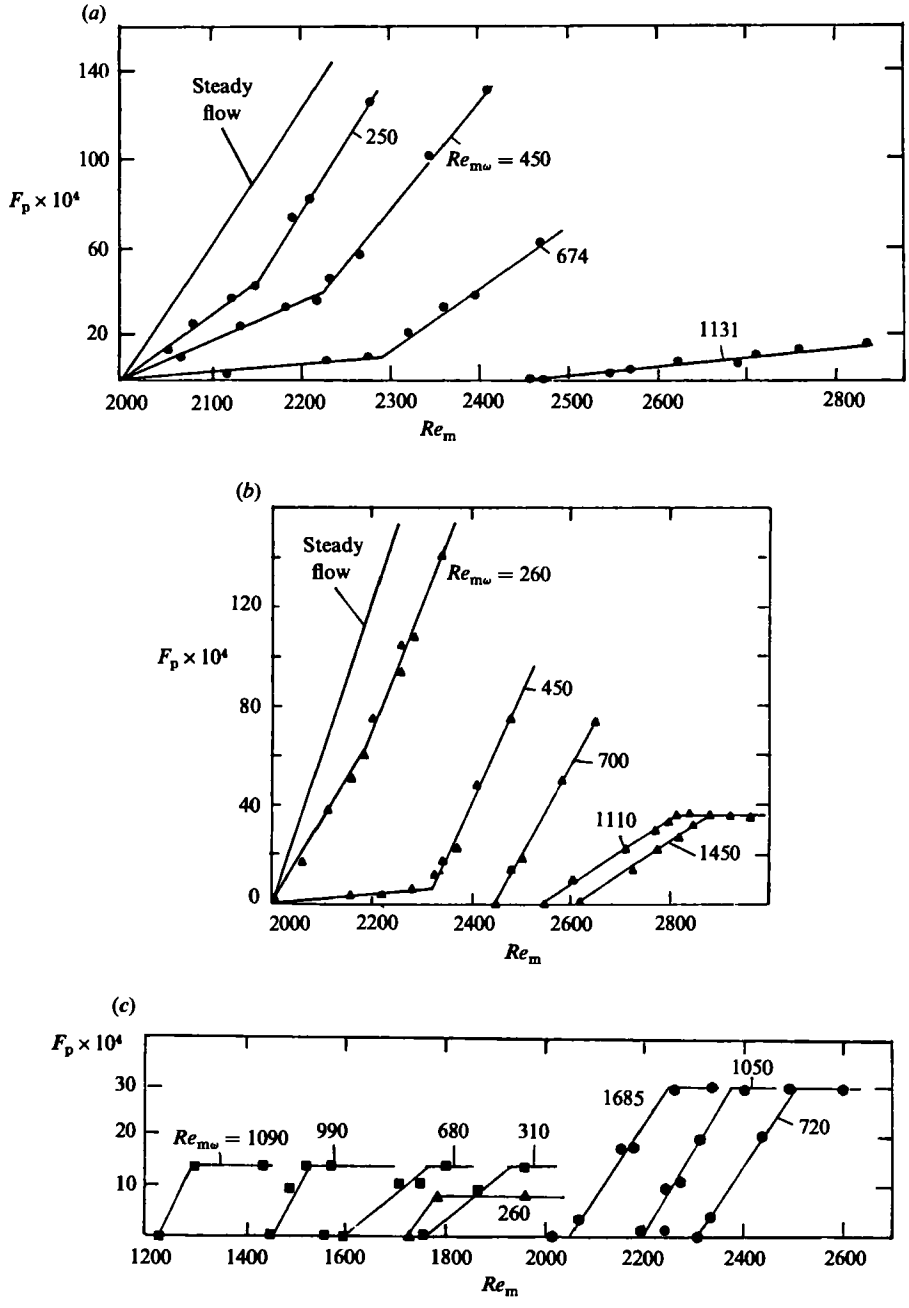

FIGURE 8 (*a–c*). For caption see following page.

velocity traces become similar to that in figure 3(*c*) is quite sensitive to small changes in the modulation amplitude. That is, the shift from phase-random to phase-locked plug formation occurs in a small but highly reproducible range of the modulation amplitude. When they occur phase-locked, small turbulent patches are observed at fairly low mean Reynolds numbers ($Re_m > 1400$). For $5 < \lambda < 10$, the F_p *vs.* Re_m curves show the same characteristic trends as the one shown in figure 8(*a*). However,

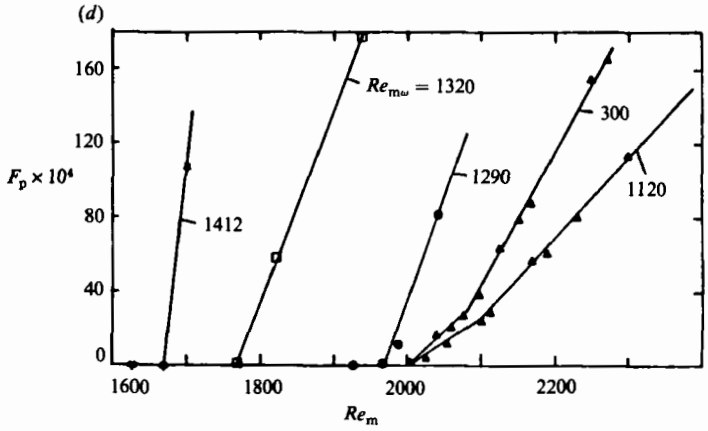

FIGURE 8. Frequency of puff as a function of mean Reynolds number Re_m. (*a*) $\lambda = 7.5$; (*b*) $\lambda = 4$; (*c*) ▲, $\lambda = 1$; ■, $\lambda = 2$; ●, $\lambda = 3.5$; (*d*) $\lambda = 33$.

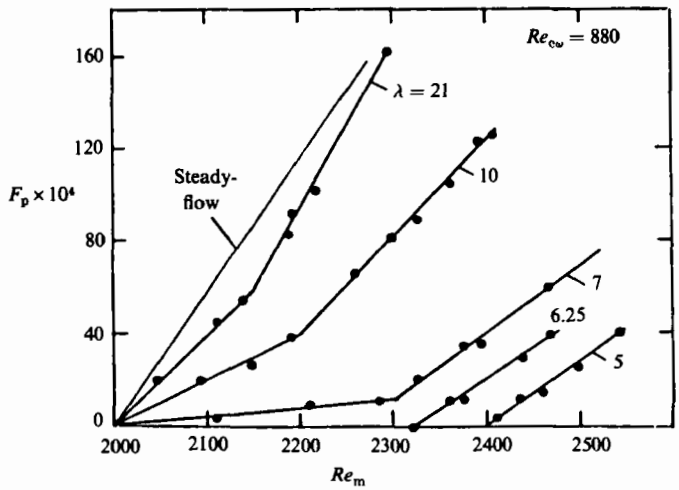

FIGURE 9. F_p–*vs.*–Re_m curves for various λ at fixed $Re_{c\omega}$ (= 880).

this is no longer the case for $\lambda = 4$ and $Re_{m\omega} > 1100$, for which the turbulent plugs start to occur at a preferred phase of each cycle (figure 8*b*).

For example, for $Re_{m\omega} = 1110$ and $Re_m < 2540$, no plugs are observed, and the flow is therefore fully laminar for all time. Increasing the mean Reynolds number Re_m results in the occurrence of small disturbances, similar to the ones shown in figure 7. Furthermore, there is a jitter in the phase at which those disturbances occur, and sometimes several cycles of fully laminar flow occur between two succeeding disturbances. Plugs occur for $Re_m > 2540$. The relative number of cycles containing a plug in each cycle increases until $Re_m \approx 2810$. There is a corresponding progressive increase in the length of the plugs and turbulent intensity. For $Re_m > 2810$ these plugs are phase locked with the flow modulation. The centreline velocity signal for this case would then be similar to the one shown in figure 5. Once a Re_m value is reached for which the plug occurs phase locked, a further increase in Re_m results in a growth in length of these turbulence patches until the flow is turbulent throughout the entire cycle of modulation, that is, the pipe flow becomes fully turbulent all the

time. The case where two or even more turbulent patches are observed during one cycle is rare.

Decreasing λ even further (i.e. for $\lambda < 3.5$) results in a decrease of the minimum modulation amplitude needed for the disturbances to occur phase locked; see figure 8(*c*). For $\lambda = 1$ and 2, patches occur phase locked at the lowest $Re_{m\omega}$ investigated (i.e. $Re_{m\omega} \simeq 300$). In figure 8(*c*), each horizontal (i.e. F_p = constant) line indicates the F_p value measured for the case of one patch per cycle. Note that the Re_m range for increase of F_p from zero to this (constant) value decreased as λ is decreased. For $\lambda = 2$ and 3.5, once the patches occur phase-locked with the flow modulation, an increase in Re_m increases the duration of these disturbances (i.e. an increase in the length of the patches), rather than their number per cycle. For the smallest λ investigated (viz. $\lambda = 1$, which corresponds to the period of oscillation of $T_p = 19$ minutes), however, an increase in the Re_m value first results in an increase in the number of turbulent patches per cycle. Eventually, at even higher Re_m, succeeding patches start to merge and interact with each other in a way very similar to plugs in steady flow (for $Re_m > 2300$). Therefore, at very low modulation frequencies, the transition from laminar flow to turbulent flow is quite similar to that observed in steady flow; that is, the flow behaves as quasi-steady, as is to be expected. It has to be mentioned that for the low frequency parameters shown in figure 8(*c*) (say $\lambda < 3.5$), the uncertainty in the F_p data is relatively high because of the rather long time needed to measure a sufficiently large number of cycles (required for stable F_p values). Hence, the measurements were aimed only at determining the maximum Re_m value for which the flow remained laminar all the time. The earlier remarks about the slopes of the F_p *vs.* Re_m curve therefore apply only qualitatively to the low λ cases. Note that for $\lambda < 3.5$, increasing $Re_{m\omega}$ decreases Re_{tr} (figure 8*c*), opposite to the trends at higher λ values (figures 8*a*, *b*). This is not unexpected because the flow is quasi-steady at low λ values, when instantaneous Re controls transition.

Figure 8(*d*) shows that at a very high modulation frequency ($\lambda = 33$), and high modulation amplitudes, the F_p *vs.* Re_m curves shift to lower Re_m values, with their slope becoming very steep with increasing $Re_{m\omega}$. In other words, the mean Reynolds number up to which the modulated flow remains laminar is decreased and the decrease is larger for a higher modulation amplitude. Note that at intermediate values (figures 8*a*, *b*), F_p *vs.* Re_m curves can be shifted to the higher Re_m range by increasing the modulation amplitude. This is not possible for very high or very low modulation frequencies (figures 8*c*, *d*). That is, increasing the modulation amplitude destabilizes the flow at high or low frequencies but stabilizes the flow at intermediate frequencies.

The effect of different modulation frequencies on the F_p–Re_m relationship is shown in figure 9. Decreasing the frequency (at a fixed $Re_{c\omega}$) has qualitatively the same effect on the F_p–Re_m curve as increasing the modulation amplitude over a certain range at a given λ (compare figures 8*a* and 9). At high λ values (figure 9) or low $Re_{m\omega}$ (figures 8*a*, *b*) the F_p–Re_m curves consist of two linear regions: a line with a lower slope at lower Re_m values. The slopes of both the linear regions decrease with either increasing amplitude of modulation at constant λ or decreasing λ values at (low) constant modulation amplitudes. Note that the slope of the second linear region can be higher than the corresponding slope for steady flow (for example, see figure 8*a* for $Re_{m\omega} = 250$ and figure 9 for $\lambda = 21$). (This has been observed for $\lambda > 5$ at low $Re_{m\omega}$.) Figure 9 shows that at $Re_{c\omega} = 880$, decreasing λ progressively stabilizes the flow until $\lambda = 5$, below which the flow is destabilized again (not shown in this figure but discussed later).

3.3. *Definition of transition Reynolds number Re_{tr} in unsteady flow*

The critical Reynolds number Re_{cr} is the value of Re below which the flow is stable to infinitesimal disturbances of all wavenumbers and frequencies. This theoretical quantity can be addressed only via controlled excitation studies, and the quantity relevant to the present study is transition Reynolds number Re_{tr}. Re_{tr} in the pipe flow is typically understood as the maximum Reynolds number Re_m for which the flow remains laminar for all time; in other words, this is the maximum Re_m value for which F_p is equal to zero. Such a definition would give for our facility the same Re_{tr} of 2000 – the steady flow value – for many of the curves shown in figures 8 and 9. The fact that flow modulation can result in a reduction of the plug passage frequency – below the steady flow value – for even low modulation amplitudes (figure 8) or high λ values (figure 9), will then not be taken into account by such a definition. For example, based on this definition, Re_{tr} would be 2000 for $Re_{m\omega} = 0$, 250, 450, or 674 in figure 8(*a*), and also for $\lambda = 0$, 7, 10, or 21 in figure 9. Furthermore, such a definition of Re_{tr} would result in a sudden jump of Re_{tr} from 2000 to a higher value when the first linear region disappears. For example, at $\lambda = 7.5$, the value of Re_{tr}, defined in such a way, will jump abruptly from 2000 to 2450 as $Re_{m\omega}$ increases above 674 (figure 8*a*). Similarly, it is clear from figure 9 that the value of Re_{tr}, if defined the same way, will jump from 2000 (at $\lambda = 7$) to 2330 (at $\lambda = 6.25$). Note that the jump in Re_{tr} will be quite abrupt between $Re_{m\omega} = 450$ and 700 in figure 8(*b*). (It is also interesting to note that the slope of the F_p–Re_m curve for $Re_{m\omega} = 1110$ in figure 8(*b*) is much steeper than that of $Re_{m\omega} = 1131$ in figure 8(*a*), demonstrating the strong influences of both λ and $Re_{m\omega}$ on F_p variations.)

Therefore, a general definition of Re_{tr} as the maximum Re_m value for which the plug frequency F_p is zero cannot be used for unsteady pipe flow. One needs to define Re_{tr} in unsteady flow in a different way. The mean Reynolds number Re_m at which the F_p *vs.* Re_m lines in figures 8, 9 show a change in their slopes seems to indicate an intrinsic change in the transition behaviour of the flow, and we define this Re_m value as the transition Reynolds number Re_{tr} for unsteady flow. This new definition, though arbitrary and lacking a rigorous basis, guarantees a continuous variation in the Re_{tr} value with $Re_{m\omega}$ at a given λ, or with λ at a given $Re_{m\omega}$. Whenever the slope of the first linear region becomes zero, Re_{tr} becomes the Re_m intercept of the F_p–Re_m line. Thus, $Re_{tr} = 2000$ becomes a special case when the flow is steady. Figure 10 shows the approximate minimum modulation amplitudes required for the first linear region to disappear. For $\lambda = 33$, an increase in $Re_{m\omega}$, above the value shown in figure 10, will not only cause the slope of the first linear region to become zero, but also shift the F_p *vs.* Re_m curves to lower Re_m, with their slopes becoming very steep (figure 8*d*). In this case, Re_{tr} will be less than 2000. Thus, the new definition of Re_{tr} appears uniformly consistent in all ranges of the controlling parameters.

3.4. *Transition boundary based on modulation amplitudes*

Following the above-introduced definition, valucs of Re_{tr} were determined from large volumes of F_p *vs.* Re_m data (similar to those shown in figures 8, 9) collected for different ranges of the unsteady flow parameters λ and $Re_{m\omega}$. These Re_{tr} data produced the laminar–transition flow boundary in the (Re_m, $Re_{m\omega}$, λ) space.

Figure 11(*a*) shows Re_{tr} as a function of the modulation amplitude $Re_{m\omega}$, parametric in λ; figure 11(*b*) presents the corresponding data in terms of Δ. For any λ in the range 3–33, Re_{tr} first increases gradually with increasing $Re_{m\omega}$ up to a point, beyond which increasing $Re_{m\omega}$ results in a decrease of Re_{tr}. The drop in Re_{tr} is

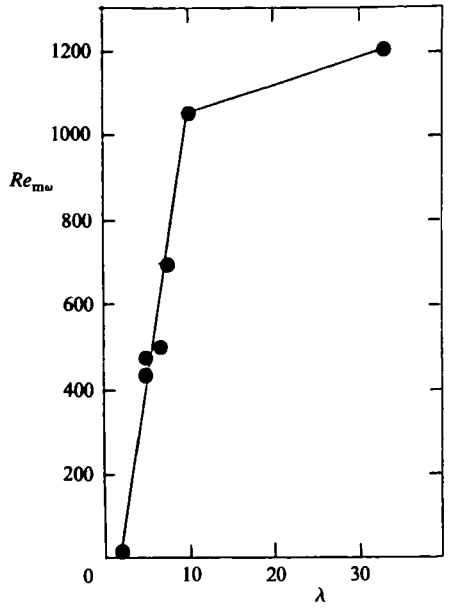

FIGURE 10. Approximate minimum modulation amplitude $Re_{m\omega}$ as a function of λ, for the slope of the first linear region of F_p *vs.* Re_m curves (see figures 9 and 10) to become zero.

extremely abrupt for $4 \leqslant \lambda \leqslant 10$, but gradual for $\lambda < 4$ or $\lambda \geqslant 33$. For very high modulation amplitudes, Re_{tr} can become even less than the steady flow value of 2000 in the λ range up to at least 33. It is interesting to recognize that this sudden decrease of Re_{tr} is associated with the change in the occurrence of plugs from being a random event in time to a phase-locked event. That is, at these high modulation amplitudes, the plugs occur phase locked with the flow excitation, and the occurrence of phase-locked plugs is accompanied by destabilization of the flow. For lower λ values (say, $\lambda \leqslant 3$) Re_{tr} is always less or equal to the Re_{tr} value of the steady flow; that is, Re_{tr} decreases with increasing values of $Re_{m\omega}$. At very low modulation frequencies ($\lambda \sim 1$), the variation of Re_{tr} with $Re_{m\omega}$ (figure 11*a*) agrees well with that expected for quasi-steady flow (see figure 12).

Note that when Δ, instead of $Re_{m\omega}$, is chosen as the amplitude parameter, the drop in the transitional Reynolds number values, as the modulation amplitude becomes very high, seems less abrupt (see figure 11*b*). Unfortunately, due to experimental restrictions, it was not possible to obtain experimental data points on the decreasing part of the $\Delta - Re_{tr}$ curves for λ values in the range 4–10. In our flow facility, it is $Re_{m\omega}$ that can be changed directly (with a minimum possible step size of about 30) and not Δ. Due to the large and abrupt decrease of Re_{tr} above a certain critical value of $Re_{m\omega}$ or Δ (figure 11*a*), the minimum possible Δ size becomes quite large.

Figure 12 illustrates three flow conditions we have to consider separately. We know that the steady flow remains fully laminar for $Re_m < 2000$. If the flow is modulated at a very low frequency ($\lambda \to 0$), then for a given $Re_{m\omega}$, turbulence will be observed only if

$$Re_m + Re_{m\omega} > 2000.$$

In addition, the flow will be turbulent only during the time interval when the

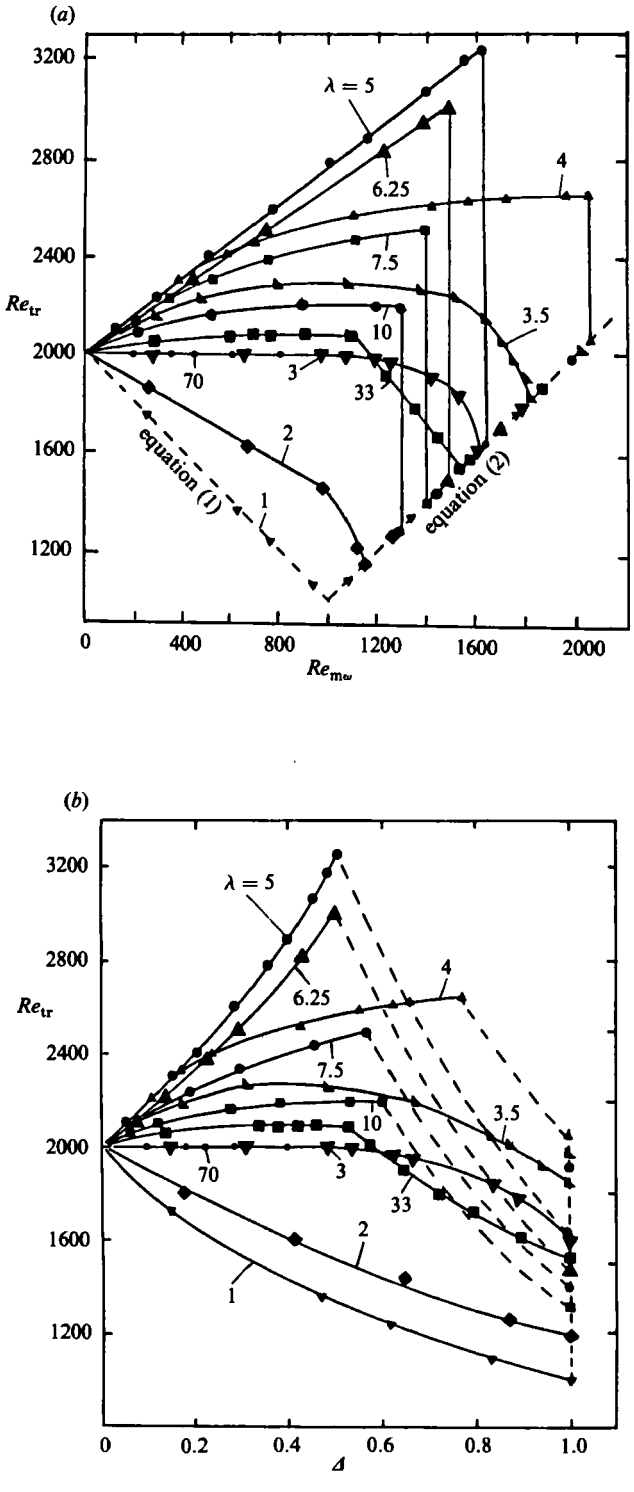

FIGURE 11. Curves separating the laminar–transition regions; (*a*) (Re_{tr}, $Re_{m\omega}$)-plane; (*b*) (Re_{tr}, Δ)-plane.

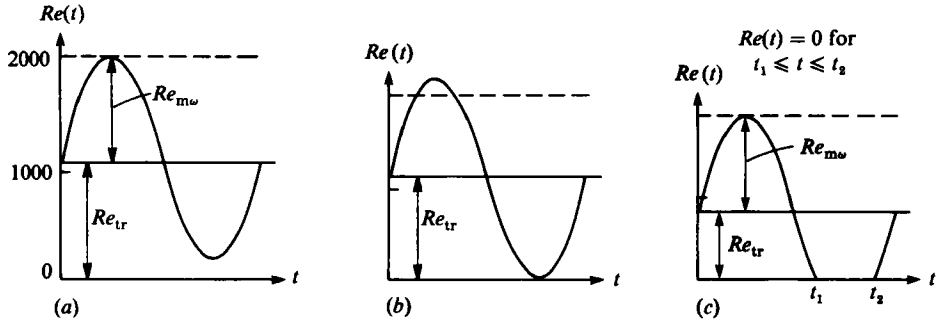

FIGURE 12. Transition Reynolds number as a function of modulation amplitude for quasi-steady flow conditions ($\lambda \to 0$). (*a*) $Re_{m\omega} < 1000$; (*b*) $Re_{m\omega} > 1000$; (*c*) $Re_{m\omega} > 1000$, with exit slot fully closed during $t_1 < t < t_2$.

instantaneous Reynolds number $Re(t) \equiv U_m(t)\, D/\nu$ is higher than 2000 (figure 12*a*). That is,

$$Re_{tr} = 2000 - Re_{m\omega}. \tag{1}$$

This equation is plotted in figure 11 (*a*), and can be viewed as a limiting case (i.e. $\lambda \to 0$). Experimental data for $\lambda = 1$ agree with this line (equation (1) in figure 11*a*).

At a modulation amplitude $Re_{m\omega} = 1000$, the (theoretical) dashed line in figure 11 (*a*) shows a change in slope of 90°. This is due to the limitation of our experimental apparatus, because instantaneous upstream flow is not permitted. Because the instantaneous cross-sectional mean velocity $U_m(t)$, hence also $Re(t)$, is always positive (being equal to zero when the exit slot is fully closed), the minimum mean Reynolds number possible is $Re_m = Re_{m\omega}$ (see figure 12*b*). For the quasi-steady model explained above, the flow is transitional at this lowest possible Re_m-value, that is,

$$Re_{tr} \leqslant Re_{m\omega} \quad \text{for } Re_{m\omega} > 1000. \tag{2}$$

(The $Re_{tr} = Re_{m\omega}$ curve is also shown in figure 11 (*a*) as equation (2).)

The experimental observations produce the unexpected result that at high enough $Re_{m\omega}$ all measured Re_{tr} *vs.* $Re_{m\omega}$ curves become identical with the theoretical curve (equation (2)); this means that turbulent plugs are observed at the minimum possible mean Reynolds number, namely at $Re_m = Re_{m\omega}$. A few measurements at high $Re_{m\omega}$ showed that turbulence occurred for flow conditions $Re_m < Re_{m\omega}$ (figure 12*c*); therefore, the actual transitional Reynolds number Re_{tr} is less than the one indicated in figure 11*a* (the true value of Re_{tr} for these cases was not measured because of the flow becoming non-sinusoidal).

3.4.1. *Comparison with theory*

A fair amount of theoretical work has been done on oscillating plane Poiseuille flows, which, for high λ values, are relevant to our experimental results. Hall (1975) found that a high-frequency oscillation slightly reduces the critical Reynolds number for all modulation amplitudes. That is,

$$\delta Re = -A^2\left(\frac{30.7}{\lambda}\right)^5, \tag{3}$$

where δRe is the percentage reduction in the critical Reynolds number due to the oscillation. His result is expected to hold for $\lambda > 71$. Von Kerczek (1982), though his results are not inconsistent with Hall's, indicates that Hall's formula is valid only for

very high λ values ($\lambda > 110$). Our experimental results show a slight increase in Re_{tr} for $\lambda \approx 33$ and $Re_{m\omega} < 1100$. For this λ value, a reduction in Re_{tr} is observed only at higher modulation amplitudes (figure 11). However, for $\lambda = 70$, quite close to the lower limit given by Hall for equation (3) to be valid, our observations show that $Re_{tr} = 2000$ for all modulation amplitudes investigated. This is also consistent with equation (3), which predicts δRe to be very small for $\Delta \leqslant 1$ when λ is large.

For intermediate and low λ values, there is no direct comparison between theoretical results on oscillating plane Poiseuille flow and our experimental data. It is nevertheless interesting to note that the theoretical analyses by Grosch & Salwen (1968), Herbert (1972) and von Kerczek (1982) showed that plane Poiseuille flow can be stabilized by oscillation if the modulation is not too large. Our data furthermore indicate an abrupt destabilization as the modulation amplitude exceeds a certain value (figure 11*b*). Such a flow destabilization at higher Δ values was also found by Grosch & Salwen in their analysis of oscillating plane Poiseuille flow, whereas von Kerczek rejects such destabilization as 'rather unlikely'. Of course, our Δ values for the observed abrupt destabilization are much larger than the values calculated by Grosch & Salwen and are also larger than the range permitted by von Kerczek's analysis.

Tozzi (1982) has theoretically investigated the stability of pulsatile flow in a circular pipe; see also Davis (1976). A comparison of these theoretical results with the experimental data of Sarpkaya (1966), Gilbrech & Combs (1963) and the present results is shown in figure 13. Only some of our results are shown in order not to overcrowd this figure. The experimentally determined critical Reynolds number Re_{cr} values of Sarpkaya (1966) and Gilbrech & Combs (1963) are based on a positive growth of small disturbances. To avoid any confusion with our transition study, we defined the change δRe in terms of the transition Reynolds number Re_{tr}, whereas they refer to theirs in terms of the critical Reynolds number Re_{cr}. Note that Sarpkaya's (1966) measurements also show a sudden decrease in Re_{cr} as Δ is increased above a certain value. In spite of the fact that our experiment on the survival of turbulent plugs is quite different from Sarpkaya's study of growth of imposed controlled perturbations, the similar trends of variations of Re_{cr} and Re_{tr} are not surprising (figure 13). This indicates that our data based on survival of plugs are perhaps quite relevant to the instability of the pipe flow.

In agreement with many other theoretical studies (e.g. Patera & Orszag 1981) Tozzi (1982) finds that the disturbance growth rate in steady pipe flow at $Re_m = 2200$ is negative, indicating laminar flow up to higher Reynolds number. Tozzi then defines the growth rate of the least stable disturbance mode of the steady flow at $Re_m = 2200$ as the 'pesudo neutral stability growth rate'. The 'critical' Reynolds number of the unsteady flow is then the maximum Re_m value for which the growth rate of the least stable mode is less than or equal to the 'pseudo neutral stability growth rate'. Such a definition makes it possible to quantify theoretically (by the δRe value) the degree of stabilization due to the oscillation (see figure 13).

All experimental laminar–transition curves (figure 13) indicate that the oscillation initially stabilizes the basic flow as the amplitude of oscillation is increased from zero. Increasing Δ above a certain value, however, results in a decrease δRe. The beginning of this descending portion of the δRe *vs.* Δ curves in figure 13 is strongly λ dependent. Gilbrech & Combs' (1963) and Tozzi's (1982) theoretical neutral stability curves and our data show the ascending portions also to be strongly λ dependent while Sarpkaya's (1966) data show virtually no λ dependence (see figure 13). The theoretical

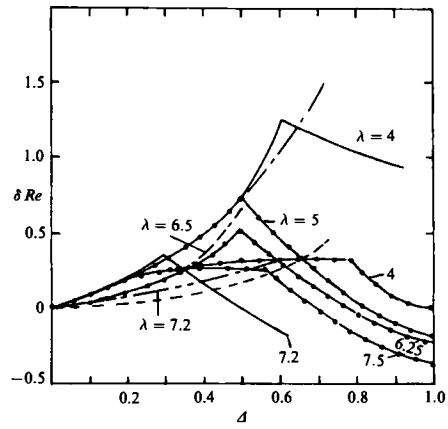

FIGURE 13. Comparison between experimental and theoretical neutral stability curves. ——, Sarpkaya (1966); — - - —, Gilbrech & Combs (1963); — · — · —, present results; – – – –, linear stability analysis, $\lambda = 5.8$, Tozzi (1982); — — —, quasi-steady-analysis, Davis (1976).

study of Tozzi, however, does not predict the descending portions of the neutral stability curves, i.e. he predicts no destabilization at higher oscillation amplitudes. Note that for the ascending portions, there is a good agreement between our data for $\lambda = 6.25$ with the $\lambda = 6.5$ curve of Gilbrech & Combs. All of our neutral stability curves fall below the curves of Sarpkaya and Davis. As already mentioned, this is to be expected in view of the difference between transition and critical Reynolds numbers Re_{tr} and Re_{cr}. Tozzi's linear stability analysis, however, indicates relatively decreased stabilization of the flow by the oscillation.

Further experimental investigations are necessary to explain the good correspondence between the ascending portions of our $\lambda = 5$ curve and the results of Sarpkaya (figure 13). Those studies, including detailed investigations of the inlet region of the pipe, should also provide some explanation for the large discrepancy between the $\lambda = 4$ data of Sarpkaya and ours.

The modulation amplitudes separating the ascending and descending portions of the laminar–transition curves (figure 11) are shown as curve *a* (with $Re_{\mathrm{m}\omega}$ ordinate) in figure 14. This curve shows that with increasing λ, the maximum $Re_{\mathrm{m}\omega}$ value which keeps the flow stable first increases and then decreases. At $\lambda = 4$, the unsteady flow remains 'stabilized' up to the highest modulation amplitude. If the frequency of oscillation is further increased (i.e. $\lambda > 4$), the transitional Reynolds number starts to decrease at already lower modulation amplitudes. Curve *b* (with $Re_{\mathrm{m}\omega}$ ordinate) in figure 14 demarcates the domain where the 'plug' occurs randomly in time (shaded area) from the domain where the plug occurs phase-locked with the excitation. Note that for λ between 6.25 and 20, curves *a* and *b* nearly coincide. In this range, the minimum oscillation amplitude necessary for phase locked occurrence of turbulent plugs is also separating the ascending and descending portions of the laminar transition curves in figure 11. At high modulation frequencies (i.e. $\lambda > 33$), the turbulent plugs occurred randomly in time even at very high modulation amplitudes, whereas at low λ they occurred phase locked at already low $Re_{\mathrm{m}\omega}$ values. This is to be expected because at low λ values the instantaneous Reynolds number $Re(t)$ should

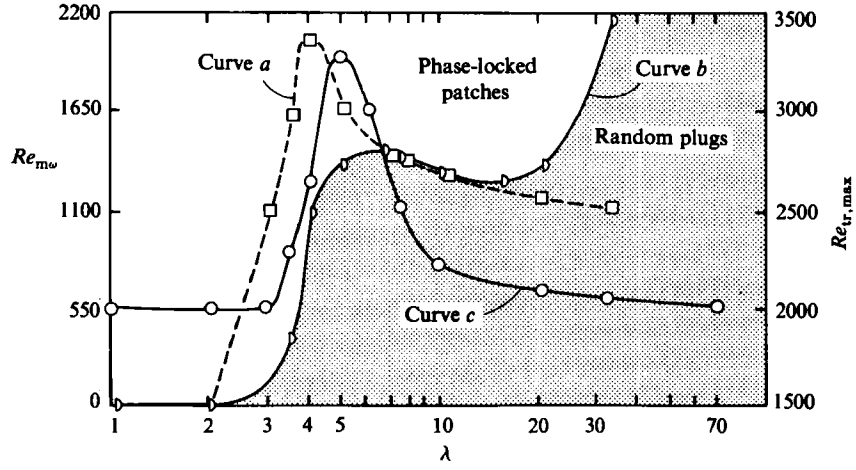

FIGURE 14. Curve a: Maximum modulation amplitudes separating the ascending and descending portions of the neutral stability curves shown in figure 11(a) ($(\lambda, Re_{m\omega})$-coordinates). Curve b: Separating flow conditions for which the turbulent 'plugs' occur randomly in time or phase locked with the flow oscillation ($(\lambda, Re_{m\omega})$-coordinates). Curve c: Maximum transition Reynolds number as a function of the oscillation frequency ($(\lambda, Re_{tr,max})$-coordinates).

be the appropriate flow parameter. At high λ values, where Re_m is the controlling parameter, the turbulent plugs occur randomly in time as in steady flow at the same mean Reynolds number. Finally, the maximum possible transition Reynolds number $Re_{tr,max}$ as a function of λ is shown in figure 14 as curve c (with $Re_{tr,max}$ ordinate). Re_{tr} is increased by about 65% over the steady flow value of 2000 at $\lambda = 5$, whereas high frequency modulations (i.e. at $\lambda > 10$) produce at most only a slight increase in Re_{tr}.

3.5. *Transition Reynolds number as a function of* λ

The effect of the frequency of modulation on Re_{tr} is shown in figure 15(a) for three $Re_{m\omega}$ values, and in figure 15(b) for three values of Δ. Note that data in figures 15(a, b) do not correspond directly. For a fixed $Re_{m\omega}$, the Re_{tr} value first increases rapidly, reaches a maximum value at $\lambda \approx 5$, then decreases to the steady flow value of 2000 at very high frequencies. At $\lambda \approx 70$, inertia forces strongly reduce the modulation amplitude. It was therefore not possible to determine Re_{tr} at $\lambda = 70$ for the highest modulation amplitude in figure 15. The decrease in Re_{tr} for λ between 5 and 10 is very rapid at high modulation amplitudes and becomes more gradual as $Re_{m\omega}$ is decreased. This rapid decrease of Re_{tr} is associated with a change in the occurrence of the plugs from being phase random at $\lambda \approx 5$ to phase-locked at $\lambda = 10$. In his paper, Sarpkaya (1966) did not present the Re_{cr} *vs.* λ stability curves. Of course, these curves can be reconstructed from his Re_{cr} *vs.* Δ data but for low Δ values only; his upper λ limit of 7.8 disallows a clear detection of the descending part of the neutral stability curves (see figure 15b), whereas for high Δ his lower λ limit of 4 disallows the ascending portion to be observed.

Increasing λ from 1 to 5 results in a rapid increase in Re_{tr} for high $Re_{m\omega}$ and Δ, but a more gradual increase for low $Re_{m\omega}$ and Δ. For unsteady flow at $\lambda \approx 3$, Re_{tr} remains about the same as for the steady flow for up to very high modulation amplitudes, all curves essentially passing through the points: $\lambda \approx 3$, $Re_{tr} \approx 2000$ (figure 15a). At $Re_{m\omega} = 1400$ and $1 < \lambda < 2$, plugs were observed at the minimum

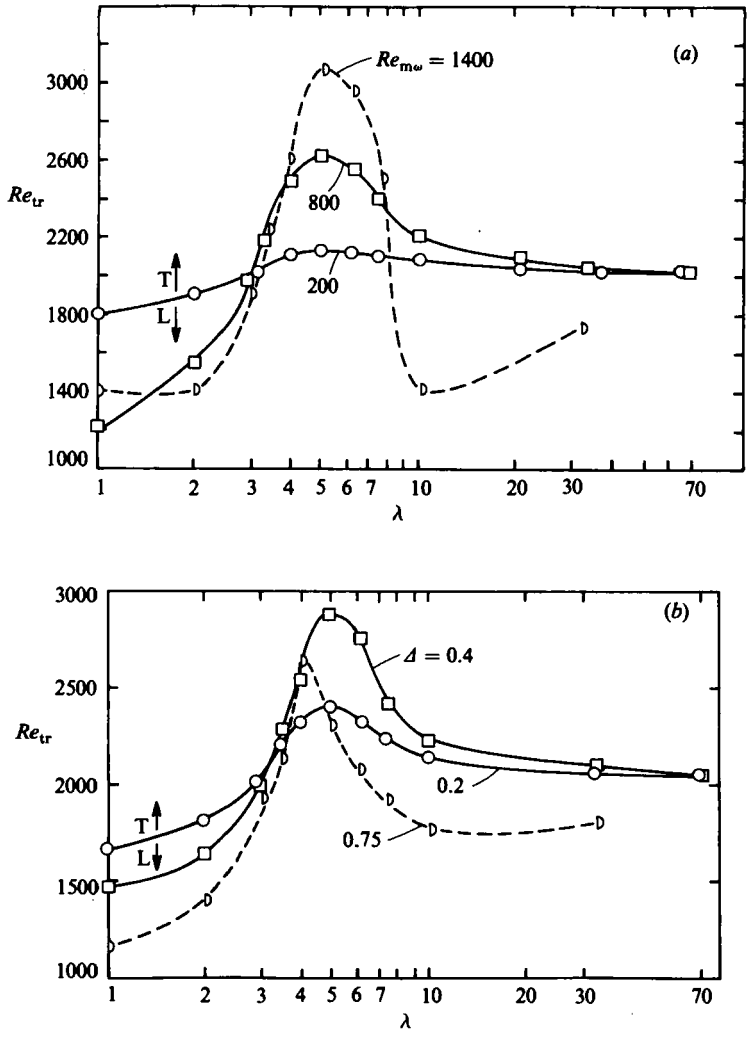

FIGURE 15. Neutral stability curves separating laminar–tranition regions in the (Re_{tr}, λ)-plane; (*a*) at constant $Re_{m\omega}$; (*b*) at constant Δ.

possible Re_m value of 1400 (see figure 12*b*), which accounts for the λ-independence of the $Re_{m\omega} = 1400$ curve in figure 15(*a*), for the $1 \leqslant \lambda \leqslant 2$ range. Note that large variations in Re_{tr} with respect to λ are confined to $1 < \lambda < 10$ (figures 15*a*, *b*) when the shape of the velocity profile is highly λ dependent; see Uchida (1956). For $\lambda > 10$, the Re_{tr} *vs.* λ become more gradual, as does the change of the velocity profile with λ.

It would be interesting to know where the λ value calculated with the frequency of the principal disturbance mode (the disturbance mode with the largest real part of the Floquet exponent (von Kerczek & Davis 1974)) falls on the Re_{tr} *vs.* λ stability curves in figure 15. Unfortunately, such a comparison is not possible as linear stability analysis of fully-developed pipe flow has, up to now, failed to prove the existence of any unstable mode.

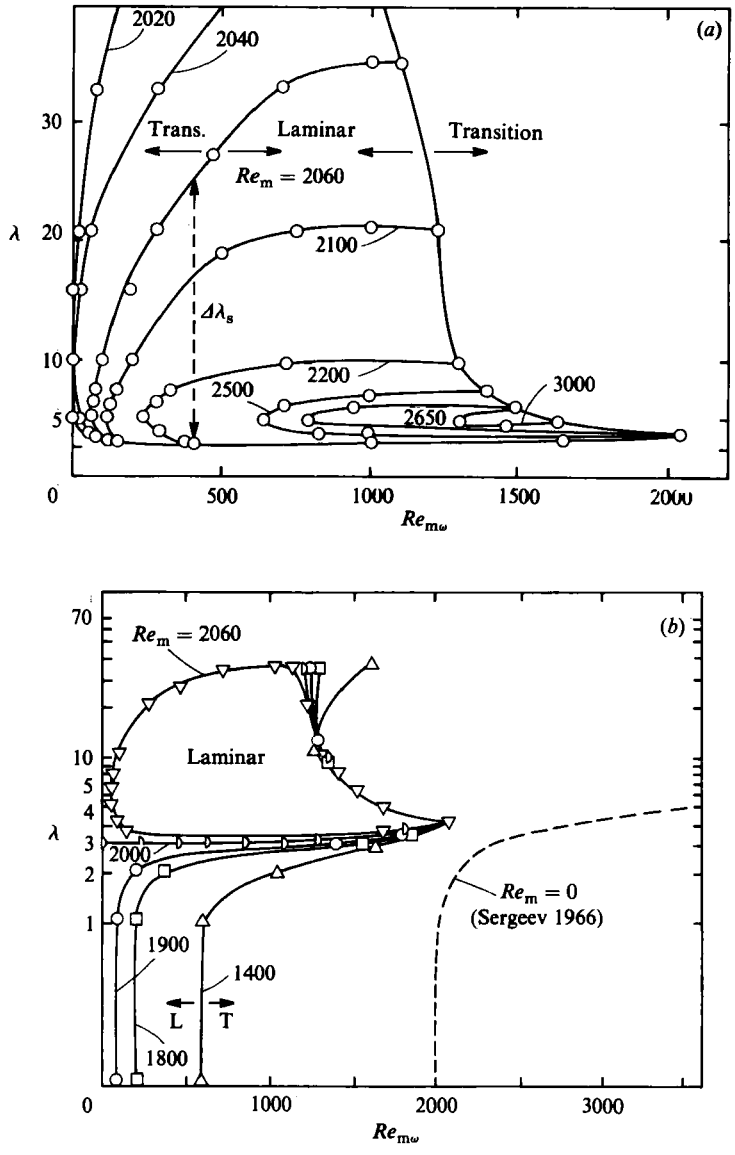

FIGURE 16 (a, c). For caption see facing page.

3.6. *Frequency bandwidth and modulation amplitude range for stability*

For a given mean Reynolds number Re_m at which the flow is otherwise unstable, modulation can stabilize the flow if the modulation frequency is within a certain bandwidth or the modulation amplitude is within a certain range. The bandwidth of frequencies that stabilizes the flow (call it stabilization bandwidth $\Delta\lambda_s$) is a strong function of Re_m and $Re_{m\omega}$. Figures 16(a)–(c) document the laminar–transition boundaries in the ($\lambda, Re_{m\omega}$)- and ($\lambda, Re_{c\omega}$)-planes, parametric in values of Re_m. For a given $Re_{m\omega}$, $\Delta\lambda_s$ decreases with increasing Re_m. For a fixed Re_m, $\Delta\lambda_s$ increases with increasing $Re_{m\omega}$ until it reaches a maximum before decreasing sharply when Re_m is low but more gradually when Re_m is high. The maximum value of the stable bandwidth $\Delta\lambda_s$ depends on Re_m, the value being lower for higher Re_m (figure 16a).

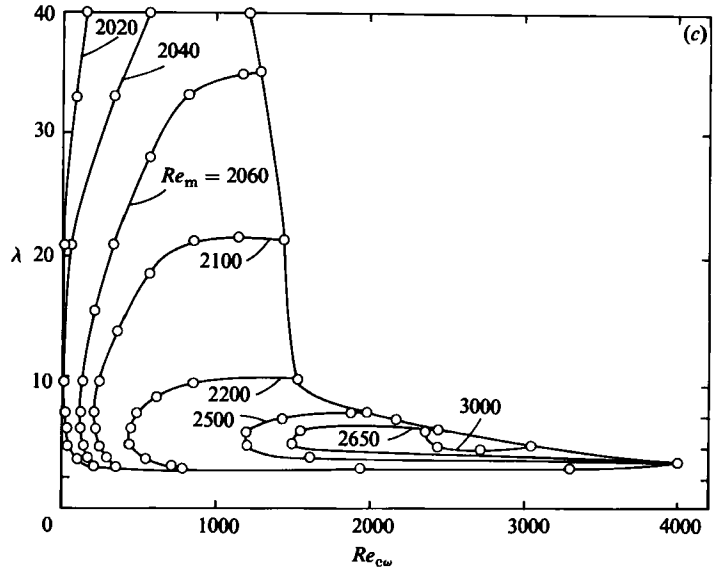

FIGURE 16. (*a*) Neutral stability curves in the $(Re_{m\omega}, \lambda)$-plane for mean Reynolds numbers above 2000. (*b*) Neutral stability curves in the $(Re_{m\omega}, \lambda)$-plane for mean Reynolds numbers below 2000. ---, Sergeev's (1966) data for $Re_m = 0$. (*c*) Neutral stability curves in the $(Re_{c\omega}, \lambda)$-plane for mean Reynolds numbers above 2000.

Note that the minimum modulation amplitude needed for the unsteady flow to be stabilized is strongly dependent on Re_m. This minimum $Re_{m\omega}$ value increases with increasing Re_m. For the limiting case $Re_m \to 2000$, the laminar–transition boundary on the left side of the closed curves in figure 16(*a*) asymptotically approaches the ordinate (i.e. the $(Re_{m\omega} = 0)$-axis). An increase in the mean Reynolds number reduces the area of the stable domain in the $(\lambda, Re_{m\omega})$-plane. Furthermore, the stable domain for a given Re_m is entirely included in that for a comparatively lower Re_m, as is to be expected.

For $Re_m = 2000$ and $\lambda \leqslant 3$, destabilization of the unsteady flow occurs over the entire $Re_{m\omega}$ range. As Re_m is decreased below 2000 – the steady-flow transition Reynolds number – destabilization occurs for $\lambda \leqslant 1$ at modulation amplitudes higher than $(2000–Re_m)$ the quasi-steady value (see figure 16*b*). As λ is increased, destabilization occurs at higher modulation amplitudes. (A logarithmic λ scale is chosen in figure 16(*b*) to emphasize the data at low λ.) Gradually decreasing the Re_m value below 2000 also results in an increase of $\Delta\lambda_s$; this bandwidth broadening increases with decreasing Re_{m_ω}. For $Re_m < 2000$, $\Delta\lambda_s$ becomes infinite as $Re_{m\omega}$ goes to zero, i.e. the flow becomes absolutely stable.

For $\lambda < 3$, gradually decreasing Re_m also results in an increase of the maximum modulation amplitude allowed for the pulsatile flow to remain laminar. Note that for $\lambda \leqslant 1$, the laminar–transition boundary becomes independent of λ, since the flow is quasi-steady in this λ-range. For $Re_m < 2000$, increasing λ from 1 to 4 results in an increase of the modulation amplitude range allowed for stability. It is interesting to note that (some of) the laminar–transition boundaries tend to merge at $\lambda \sim 4$, $Re_{m\omega} \approx 2050$.

With decreasing Re_m at a given $Re_{m\omega}$, the flow should progressively approach the Stokes layer. Data for $Re_m = 0$ by Sergeev (1966) are also included in figure 16(*b*). In our case, we could not cover extensive Re_m data for we were limited to the

$Re_{m\omega} \leqslant Re_m$ range because of apparatus limitations. It will be quite interesting to cover the cases of $Re_m < Re_{m\omega}$ and see how the laminar–transition boundary changes in the limit $Re_m \to 0$. The low Re_m cases are also relevant to human arterial flows (Stettler, Niederer & Anliker 1981).

As in Stokes layers, the modulation amplitude of the free stream (say, centreline) velocity may be more interesting than the modulation amplitude of the cross-sectional mean flow. With this in mind, the laminar–transition boundary is thus shown in the $(\lambda, Re_{c\omega})$-plane for various Re_m values (figure 16*c*). Qualitatively, these curves show the same trends as the one shown in figure 16(*a*); they are included for completeness.

This research was funded by the Office of Naval Research under Grant N00014-85-K-0126. We are grateful to Drs Bob Whitehead and Mike Reischman for continuing encouragement and to Dr K. B. M. Q. Zaman for his help in recording the data of figure 5 with an on-line laboratory computer.

REFERENCES

ANLIKER, M., CASTY, M., FRIEDLI, P., KELLER, H. & KUBLI, R. 1977 In *Cardiovascular Flow Dynamics and Measurements* (ed. N. H. C. Hwang & N. Normann). Baltimore, MD: University Park Press.

BANDYOPADHYAY, P. & HUSSAIN, A. K. M. F. 1985 In *Flow Visualization III* (ed. W. J. Yang), p. 521. Hemisphere..

BENNEY, D. J. & BERGERON, R. F. 1969 *Stud. Appl. Maths* **48**, 181.

BROWN, S. N. & STEWARTSON, K. 1980 *Geophys. Astrophys. Fluid Dyn.* **16**, 171.

CANTWELL, B. 1981 *Ann. Rev. Fluid Mech.* **13**, 457.

COLES, D. 1981 *Proc. Indian Acad. Sci.* (Engng Sci.) **4**, 111.

DAVEY, A. & DRAZIN, P. G. 1969 *J. Fluid Mech.* **36**, 209.

DAVEY, A. & NGUYEN, H. P. F. 1971 *J. Fluid Mech.* **45**, 701.

DAVIS, R. E. 1969 *J. Fluid Mech.* **36**, 337.

DAVIS, S. H. 1976 *Ann. Rev. Fluid Mech.* **8**, 57.

DRAZIN, P. G. & REID, W. H. 1981 *Hydrodynamic Stability*. Cambridge University Press.

GARG, V. K. & ROULEAU, W. T. 1972 *J. Fluid Mech.* **54**, 113.

GILBRECH, D. A. & COMBS, G. O. 1963 In *Developments in Theoretical and Applied Mechanics*, vol. I, p. 292. Plenum.

GILL, A. E. 1965 *J. Fluid Mech.* **21**, 503.

GILL, A. E. 1973 *J. Fluid Mech.* **61**, 97.

GREENSPAN, H. P. & BENNEY, D. J. 1963 *J. Fluid Mech.* **15**, 133.

GROSCH, C. E. & SALWEN, H. 1968 *J. Fluid Mech.* **34**, 177.

HABERMAN, R. 1972 *Stud. Appl. Maths* **51**, 139.

HALL, P. 1975 *Proc. R. Soc. Lond.* A **344**, 453.

HERBERT, D. M. 1972 *J. Fluid Mech.* **56**, 73.

HINO, M., SAWAMOTO, M. & TAKASU, S. 1976 *J. Fluid Mech.* **75**, 193.

HOCKING, L. M. 1977 *Q. J. Mech. Maths* **30**, 343.

HUSSAIN, A. K. M. F. 1977 In *Cardiovascular Flow Dynamics and Measurements* (ed. N. H. C. Hwang & N. Normann), p. 541. Baltimore, MD: University Park Press.

ITOH, N. 1977 *J. Fluid Mech.* **82**, 469.

KERCZEK, C. H. VON & DAVIS, S. H. 1974 *J. Fluid Mech.* **62**, 753.

KERCZEK, C. H. VON 1982 *J. Fluid Mech.* **116**, 91.

LANDAHL, M. T. 1967 *J. Fluid Mech.* **29**, 441.

LEITE, R. J. 1959 *J. Fluid Mech.* **5**, 81.

LEITKO, A. D. & HUSSAIN, A. K. M. F. 1983 *Bull. Am. Phys. Soc.* **28**, 1402.

LESSEN, M., SADLER, S. G. & LIU, T. Y. 1968 *Phys. Fluids* **11**, 1404.

LIN, C. C. 1955 *The Theory of Hydrodynamic Stability*. Cambridge University Press.

LINDGREN, E. R. 1957 *Ark. Fys.* **12**, 1.

MACKRODT, P. A. 1976 *J. Fluid Mech.* **73**, 153.

MERKLI, P. & THOMANN, H. 1975 *J. Fluid Mech.* **68**, 567.

MORKOVIN, M. V. 1977 *AGARDograph* no. 236.

NEREM, R. M. & SEED, N. A. 1972 *Cardiovascular Res.* **6**, 1.

PATERA, A. T. & ORSZAG, S. A. 1981 *J. Fluid Mech.* **112**, 467.

RAMAPRIAN, B. R. & TU, S. W. 1980 *J. Fluid Mech.* **100**, 513.

REYNOLDS, W. C. & HUSSAIN, A. K. M. F. 1972 *J. Fluid Mech.* **54**, 263.

ROSENBLAT, S. & DAVIS, S. H. 1979 *SIAM J. Appl. Maths* **37**, 1.

ROSHKO, A. 1976 *AIAA J.* **10**, 1349.

ROTTA, J. 1956 *Ing. Arch.* **24**, 258.

RUBIN, Y., WYGNANSKI, I. & HARITONIDIS, J. H. 1980 In *IUTAM Symp. on Laminar Turbulent Transition* (ed. R. Eppler & H. Fasel), p. 17. Springer.

SARPKAYA, T. 1966 *Trans. ASME* D: *J. Basic Engng* **88**, 589.

SCHULTZ-GRUNOW, F. 1940 *Forschung* **11**, 170–187, (NASA Tech. Transl. NASA-TT-F-14881, 1973).

SERGEEV, S. I. 1966 *Fluid Dyn.* (Mekh 2H) **1**, 21.

SHEMER, I. & WYGNANSKI, I. 1981 *3rd symp. on turbulent shear flows, University of California.* Davis.

SMITH, F. T. 1979 *Mathematika* **26**, 187.

SMITH, F. T. & BODONYI, R. J. 1982 *Proc. R. Soc. Lond.* A **384**, 463.

STETTLER, J. C., ZAMAN, K. B. M. Q. & HUSSAIN, A. K. M. F. 1986 *J. Fluid Mech.* (in preparation).

STETTLER, J. C., NIEDERER, P. & ANLIKER, M. 1981 *Ann. Biomed. Engng* **9**, 145.

STUART, J. T. 1960 *J. Fluid Mech.* **9**, 352.

TATSUMI, T. 1952 *J. Phys. Soc. Japan* **1**, 489.

TOZZI, J. T. 1982 Ph.D. thesis, Catholic University.

UCHIDA, S. 1956 *Z. angew. Math. Phys.* **7**, 403.

WATSON, J. 1960 *J. Fluid Mech.* **9**, 371.

WYGNANSKI, I. J. & CHAMPAGNE, F. H. 1973 *J. Fluid Mech.* **59**, 281.

WYGNANSKI, I., SOKOLOV, M. & FRIEDMAN, D. 1975 *J. Fluid Mech.* **69**, 283.

YELLIN, E. L. 1966 *Circulation Res.* **19**, 791.